

Evolution of the Fermi surface with carrier concentration in $\text{Bi}_2\text{Sr}_2\text{CaCu}_2\text{O}_{8+\delta}$

H. Ding,^{1,2} M. R. Norman,² T. Yokoya,³ T. Takeuchi,^{2,4} M. Randeria,⁵ J. C. Campuzano,^{1,2} T. Takahashi,³ T. Mochiku,⁶ and K. Kadowaki^{6,7}

(1) *Department of Physics, University of Illinois at Chicago, Chicago, IL 60607*

(2) *Materials Sciences Division, Argonne National Laboratory, Argonne, IL 60439*

(3) *Department of Physics, Tohoku University, 980 Sendai, Japan*

(4) *Department of Crystalline Materials Science, Nagoya University, Nagoya 464-01, Japan*

(5) *Tata Institute of Fundamental Research, Bombay 400005, India*

(6) *National Research Institute for Metals, Sengen, Tsukuba, Ibaraki 305, Japan*

(7) *Institute of Materials Science, University of Tsukuba, Ibaraki 305, Japan*

We show, by use of angle-resolved photoemission spectroscopy, that underdoped $\text{Bi}_2\text{Sr}_2\text{CaCu}_2\text{O}_{8+\delta}$ appears to have a large Fermi surface centered at (π, π) , even for samples with a T_c as low as 15 K. No clear evidence of a Fermi surface pocket around $(\pi/2, \pi/2)$ has been found. These conclusions are based on a determination of the minimum gap locus in the pseudogap regime $T_c < T < T^*$, which is found to coincide with the locus of gapless excitations in momentum space (Fermi surface) determined above T^* . These results suggest that the pseudogap is more likely of precursor pairing rather than magnetic origin.

PACS numbers: 71.25.Hc, 74.25.Jb, 74.72.Hs, 79.60.Bm

One of the most significant facts that has been learned about high temperature superconductors with optimal doping (highest T_c) is that they possess a large Luttinger Fermi surface containing $1+x$ holes, where x is the number of doped holes, rather than x . This has been clearly established now for a number of cuprates by use of angle-resolved photoemission spectroscopy (ARPES), including YBCO [1], BSCCO [2,3], and NCCO [4]. Fewer studies exist on underdoped cuprates [5]. Recently, the Stanford group [6] and our own group [7] have presented data on underdoped BSCCO. These data are quite remarkable in that they show the existence of a highly anisotropic (d-wave-like) pseudogap which persists up to a temperature T^* that can be significantly higher than T_c [7].

In this paper, we address in detail the question of the evolution of the Fermi surface with doping. In lightly underdoped samples, where T^* is low enough, we determine the Fermi surface – the locus of points in momentum space with gapless excitations – above T^* where the pseudogap has vanished. We find that this coincides with the locus of minimum excitation gap in the pseudogap regime ($T_c < T < T^*$). In the highly underdoped low T_c samples, T^* is too high, so we have to infer a Fermi surface from the minimum gap locus in the pseudogap regime. For all doping values studied, we find a large Fermi surface whose volume is consistent with $1+x$ holes.

The experiments were carried out at the Synchrotron Radiation Center following procedures described previously [7,8]. Underdoping was achieved by adjusting the oxygen partial pressure during annealing the float-zone grown crystals. These crystals have sharp x-ray diffraction rocking curves with structural coherence lengths similar to the near-optimally doped samples studied ear-

lier. All samples show a very flat surface after cleaving, which is essential for determining the Fermi surface. We have studied several samples ranging from overdoped to underdoped (optimal doping corresponds to a 92K T_c); in this paper we will focus on a moderately underdoped sample with a 83K T_c (transition width 2 K), and a heavily underdoped sample with T_c of 15K (width > 5 K), and contrast these results with a slightly overdoped 87K sample (width 1K). We will label the samples by their onset T_c 's.

The first point to address is how to determine the Fermi surface. Typically in ARPES, one measures energy distribution curves (EDCs) at several k points along various directions in momentum space. Along a cut moving from occupied to unoccupied states, a broad spectral peak in the EDC at high binding energy moves to lower binding energy and narrows as the Fermi crossing is approached. For $k > k_F$, the spectral weight of the peak then drops off. The Fermi crossing is usually characterized by where the intensity of the peak has been reduced by half. A more proper definition [9] is to realize that if a spectral function interpretation of the EDC is correct, then by integrating the EDC over energy, one obtains the momentum distribution function, $n_{\vec{k}}$. k_F is then defined to be where $|\nabla n_{\vec{k}}|$ is maximal. We have shown, at least along certain cuts in momentum space, that this procedure works for both YBCO and BSCCO [9,10]. However, we have found that background emission, superlattice effects, and \vec{k} -dependent matrix elements can complicate the identification of integrated EDCs with $n_{\vec{k}}$.

A simpler way to characterize the Fermi surface is to track the evolution of the leading edge of the EDC. If all EDCs along a cut are plotted on top of one another (see Fig. 1a), then as one moves from occupied to un-

occupied states, the leading edge moves to low binding energy, then moves back to higher binding energy. A similar behavior is found in simulations which take into account the experimental dispersion and resolution, with the moving back of the leading edge due to a drop of spectral intensity as k goes beyond k_F . The simulations find that the EDC just before the leading edge moves back agrees with the actual Fermi crossing to within half the k -resolution. The Fermi crossing determined this way typically coincides with the point where the leading edge has the sharpest slope and whose midpoint has moved to the lowest binding energy. This criterion has the advantage of being well-defined even when an excitation gap is present, in which case it defines the minimum gap locus. We note that in a superconductor the minimum gap locus coincides with the normal state Fermi surface [11,10]. This would not be the case if the gap were due to a charge or spin density wave, since in that case the minimum gap locus is determined by the q vector of the instability, which would only coincide with the Fermi surface if one had perfect nesting.

In Fig. 1a we show EDCs from two representative cuts in the zone for the 83K sample at $T = 160\text{K}$. Since the pseudogap closes at $T^* \simeq 170\text{K}$ for this sample [7], these data essentially represent the gapless state. We note that the spectra are very broad, a consequence of self-energy effects further enhanced by the elevated temperature. In effect, there are no well-defined quasiparticles at this temperature. Despite this, we clearly see dispersion and infer Fermi crossings, where for $k > k_F$, the spectral intensity decreases and the leading edge pulls back. The solid triangles plotted in Fig. 1c represent our estimate of the Fermi surface which is similar to that for optimally doped samples [8,3,12]. Most importantly, we infer a Fermi crossing along the $\bar{M} - Y$ ($\pi, 0 - \pi, \pi$) direction.

Several cuts normal to the Fermi surface have been measured in the pseudogap regime at 90K, just above T_c but well below T^* . In the left panel of Fig. 1b we plot EDCs for one of these cuts, and show that the leading edge evolution is similar to that of Fig. 1a, the difference being the presence of an excitation gap at 90 K. In the right panel, we plot the midpoint shift of the leading edge of the spectrum and its width along this cut (determined by fitting the leading edge to a Fermi function, the width being the effective temperature of the fit). Both the midpoint shift and the width of the leading edge have a minimum value at the same location along a cut, which defines the minimum gap locus. As shown in Fig. 1c, this locus coincides with the Fermi surface above T^* within experimental error bars.

In Fig. 2a we show EDCs from one of seven cuts (labeled I in Fig. 2c) for the 15K sample at $T=15\text{ K}$, which shows strong dispersive effects even in this highly underdoped sample. The resulting minimum gap locus from these cuts is shown in Fig. 2c. This locus is similar to that of the 83K sample shown in Fig. 1c, and we find no evi-

dence for a small hole pocket centered about $(\pi/2, \pi/2)$. To further test this, we took a cut (labeled II in Fig. 2c) along $\bar{M} - Y/2$ ($\pi, 0 - \pi/2, \pi/2$), whose EDCs are shown in Fig. 2b. If a pocket existed, then one would observe a gapless point along this cut. However a large gap is found at all points, inconsistent with the existence of a Fermi crossing. A plot of the leading edge midpoints along the minimum gap locus is similar to that of a 10K sample shown in our earlier work [7], indicating the presence of a highly anisotropic gap. The gap monotonically increases from the (π, π) direction, but the behavior around the node is flattened relative to a simple d-wave gap. This flattening might suggest that the highly underdoped materials actually possess a gapless Fermi arc [6]. However, as explained above, there is no evidence for the closing of this arc, or for a shadow-band feature in the dispersion. A more likely explanation is that the increased linewidth broadening in the underdoped material is responsible for this flattening near the node (e.g., for Lorentzian broadening, the midpoint shift is equal to the actual gap minus Γ), and that this small gap region is just part of a large minimum gap locus which intersects $\bar{M} - Y$. We note that it becomes increasingly difficult to determine the actual minimum gap locus in a region near the \bar{M} point as the sample becomes increasingly underdoped. This is because of the small dispersion near this point, which occurs even for optimal doping, and the strong drop of the signal relative to background emission as the doping decreases. However, our data indicate that the leading edge evolution along cuts near \bar{M} in the underdoped samples is similar to that at optimal doping and consistent with the existence of a large minimum gap locus, which we identify with the Fermi surface underlying the pseudogap state.

In Fig. 3 we plot the Fermi surfaces for the 87K, 83K, and 15K samples. We emphasize that a large surface is found in all three cases, similar to results obtained for underdoped YBCO [5]. Also plotted in Fig. 3 are the predicted surfaces based on a rigid band shift relative to the 87K sample for doping values of 18% (87K), 13% (83K), and 6% (15K). It is apparent from Fig. 3 that the experimental error bars do not permit us to determine the changes in area enclosed by the Fermi surface, and thus to deduce the hole doping x . The error bars are due to determining the Fermi crossings as well as the alignment of the samples.

We now turn to the issue of sample aging. BSCCO has a natural cleavage plane due to weak van der Waals coupling of the two BiO layers. The BiO surface in optimally doped samples is relatively inert to the residual gases in the vacuum chamber ($5 \cdot 10^{-11}$ Torr), and a clean surface can be regenerated by warming the sample above 50 K. However, we have found this not to be the case in our underdoped samples. In particular, after a day in the chamber, the quasiparticle peak at low temperatures becomes narrower and stronger as illustrated in Fig. 4a,

where we show the spectrum of the 83K sample measured at \bar{M} for a newly cleaved surface (blue line) and after 41 hours (red line), with an 87K spectrum (black line) plotted for comparison. This is in contrast with expected behavior of surface contamination which would lead to a broader peak due to scattering of the photoelectrons off adsorbed gases. In fact, the spectrum of the aged 83K sample becomes similar to that of the 87K sample. This leads us to speculate that the underdoped BSCCO surface's doping level has increased. Another important finding from Fig. 4a is that the whole spectrum shifts toward the Fermi energy. The shift in the main valence band below 1 eV is about 40 meV which suggests a rigid band shift due to an increase in the doping level. Also, the aging behavior of underdoped BSCCO supports the claim that the broadness of quasiparticle peaks is due to underdoping rather than impurities [7]. Similar behavior is seen in the 15K sample, where the aged spectra show a sharper leading edge. In fact, the leading edge behavior of the aged 15K sample clearly shows that the Fermi surface expands with aging in support of an increase in the doping level, as plotted in Fig. 2c. All data presented in Figs. 1-3 are obtained within a short period of time after cleaving, ensuring that intrinsic spectra were measured.

Finally, we consider the theoretical implications of this work. The coincidence of the Fermi surface with the minimum gap locus is in support of a precursor pairing gap interpretation of the pseudogap [13,14], but the present data cannot distinguish between pairing of neutral spinons versus real electrons. We should remark that a simple mean-field simulation of a magnetic gap has a minimum gap location along $\bar{M} - Y$, which does coincide with the paramagnetic Fermi crossing. On the other hand, this gap is around 200 meV if one requires a small hole pocket with the desired size ($x=0.06$). Moreover, the occupied band along this direction is a shadow band (the main band being pushed above the Fermi energy). This is inconsistent with the fact that no evidence of the shadow band is seen along $\Gamma - Y$. We should remark that Marshall et al [6] claim the existence of an energy scale at about 200 meV near \bar{M} in underdoped samples. In our opinion, this is simply associated with the incoherent part of the spectral function. A similar effect is seen in optimally doped samples at low T due to the low frequency suppression of the imaginary part of the self-energy caused by the superconducting gap, which produces a higher binding energy hump in the spectrum separate from the quasiparticle peak [9]. In the normal state, this energy scale is no longer apparent since the gapping effect is removed, and the spectral peak location in the normal state is consistent with a small binding energy (Fig. 2, Ref. [9]). To illustrate this further, we show in Fig. 4b data from an underdoped 60K sample near \bar{M} . The unaged EDC shows a feature near 200 meV, but also clearly shows, at a much lower binding energy, a sharp leading edge with a midpoint of 20 meV. As the sample

ages, the 200 meV feature moves up in binding energy (becoming the hump in optimally doped samples), and the sharp leading edge evolves into a quasiparticle peak. [15]

In conclusion, we find a large Fermi surface for underdoped BSCCO samples, even with a T_c as low as 15 K. No evidence is found for small hole pockets. Moreover, we have shown, at least in an 83K sample, that the minimum gap locus in the pseudogap phase coincides with the Fermi surface determined in the normal state above T^* . This supports the idea that the pseudogap is of precursor pairing rather than magnetic origin.

This work was supported by the U. S. Dept. of Energy, Basic Energy Sciences, under contract W-31-109-ENG-38, the National Science Foundation DMR 9624048, and DMR 91-20000 through the Science and Technology Center for Superconductivity, the Japan Society for the promotion of Science, NEDO, and the Ministry of Education, Science and Culture of Japan. The Synchrotron Radiation Center is supported by NSF grant DMR-9212658.

-
- [1] J. C. Campuzano *et al.*, Phys. Rev. Lett. **64**, 2308 (1990).
 - [2] C. G. Olson *et al.*, Phys. Rev. **B42**, 381 (1990).
 - [3] H. Ding *et al.*, Phys. Rev. Lett. **76**, 1533 (1996).
 - [4] D. M. King *et al.*, Phys. Rev. Lett. **70**, 3159 (1993); R. O. Anderson *et al.*, Phys. Rev. Lett. **70**, 3163 (1993).
 - [5] R. Liu *et al.*, Phys. Rev. **B45**, 5614 (1992) and **B46**, 11056 (1992).
 - [6] D. S. Marshall *et al.*, Phys. Rev. Lett. **76**, 4841 (1996); A. G. Loeser *et al.*, Science **273**, 325 (1996).
 - [7] H. Ding *et al.*, Nature **382**, 51 (1996).
 - [8] H. Ding *et al.*, Phys. Rev. Lett. **74**, 2784 (1995).
 - [9] M. Randeria *et al.*, Phys. Rev. Lett. **74**, 4951 (1995).
 - [10] J. C. Campuzano *et al.*, Phys. Rev. **B53**, 14737 (1996).
 - [11] J. R. Schrieffer, *Theory of Superconductivity* (W. A. Benjamin, New York, 1964).
 - [12] H. Ding *et al.* Phys. Rev. **B54**, 9678 (1996).
 - [13] M. Randeria *et al.*, Phys. Rev. Lett. **69**, 2001 (1992); N. Trivedi and M. Randeria, Phys. Rev. Lett. **75**, 312 (1995).
 - [14] T. Tanamoto, H. Kohno, and H. Fukuyama, J. Phys. Soc. Japan **61**, 1886 (1992).
 - [15] We do not see a sharp quasiparticle peak in the unaged spectrum of the 60K sample, even at 14K. This may be due to the very broad transition width of this sample.

FIG. 1. Measurements of the 83K sample. Fig. 1a: EDCs at a photon energy of 19 eV at 160K along cuts I, II in Fig. 1c. Fig. 1b: EDCs at a photon energy of 22 eV at 90K along cut III in Fig. 1c (left panel). Midpoint shifts (blue dots) and widths (red diamonds) of this cut (right panel). Fig. 1c: Fermi surface (FS) at 160K (solid blue triangles) and minimum gap locus (MGL) at 90K (solid red dots). Cuts I, II (open blue triangles) and cut III (open red dots) are locations of EDCs in Fig. 1a and b. Notice that the two surfaces coincide within error bars. The error bars represent uncertainties of Fermi crossings as well as possible sample misalignment. The red curve is a rigid band estimate of the Fermi surface.

FIG. 2. Measurements of the 15K sample at a photon energy of 22 eV at 15K. Fig. 2a: EDCs along cut I in Fig. 2c. The red curve is the Fermi crossing, and the blue ones umklapps due to the superlattice [3]. Fig. 2b: EDCs along cut II in Fig. 2c. Note that a gap is present for all EDCs from this cut. Fig. 2c: The minimum gap locus (solid red dots). Solid blue triangles represent the minimum gap locus after the sample has aged, indicating an increased doping (for visual clarity, it is shown only near the (π, π) direction). Open dots and triangles represent the cuts from Fig. 2a and b (with solid blue dots marking the umklapp locations).

FIG. 3. Fermi surfaces of the 87K, 83K, and 15K samples (error bars are similar to Figs. 1c and 2c). All surfaces have a large volume. The solid lines are tight binding estimates of the Fermi surface at 18%, 13%, and 6% doping assuming rigid band behavior.

FIG. 4. Aging effects ($T=14K$). Fig. 4a: EDCs of the 83K sample at \bar{M} for a newly cleaved surface (blue line) and after 41 hours (red line), with the EDC of the 87K sample (black line) plotted for comparison. The 40 meV shift is between the leading edges of the main valence bands of the two 83K spectra. Fig. 4b: EDC of the 60K sample near \bar{M} for an unaged surface (blue line) and an aged surface (red line). Note the 200 meV hump moves to lower binding energy, and the low binding energy leading edge evolves into a quasiparticle peak.

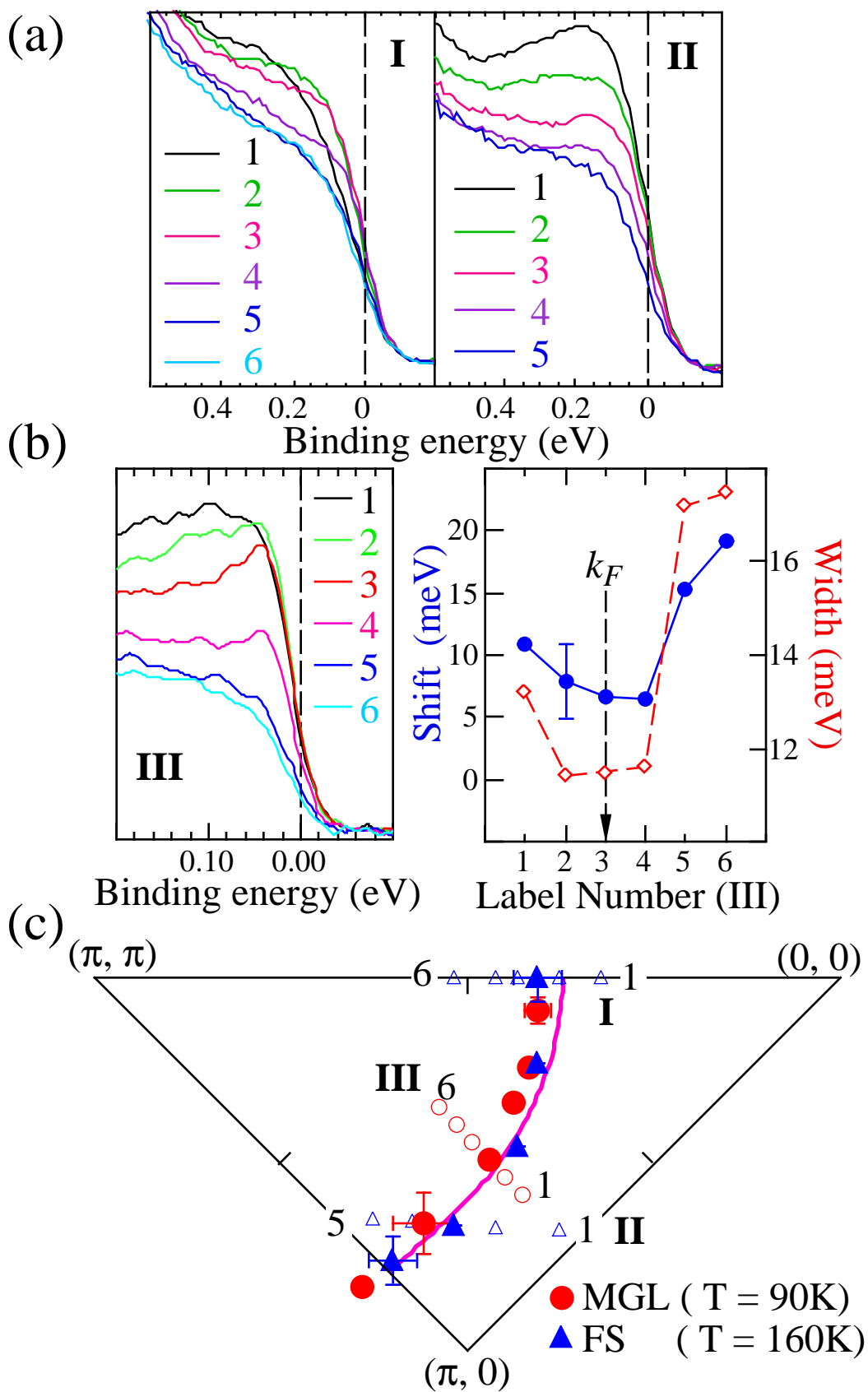


Figure 1 Ding et al.

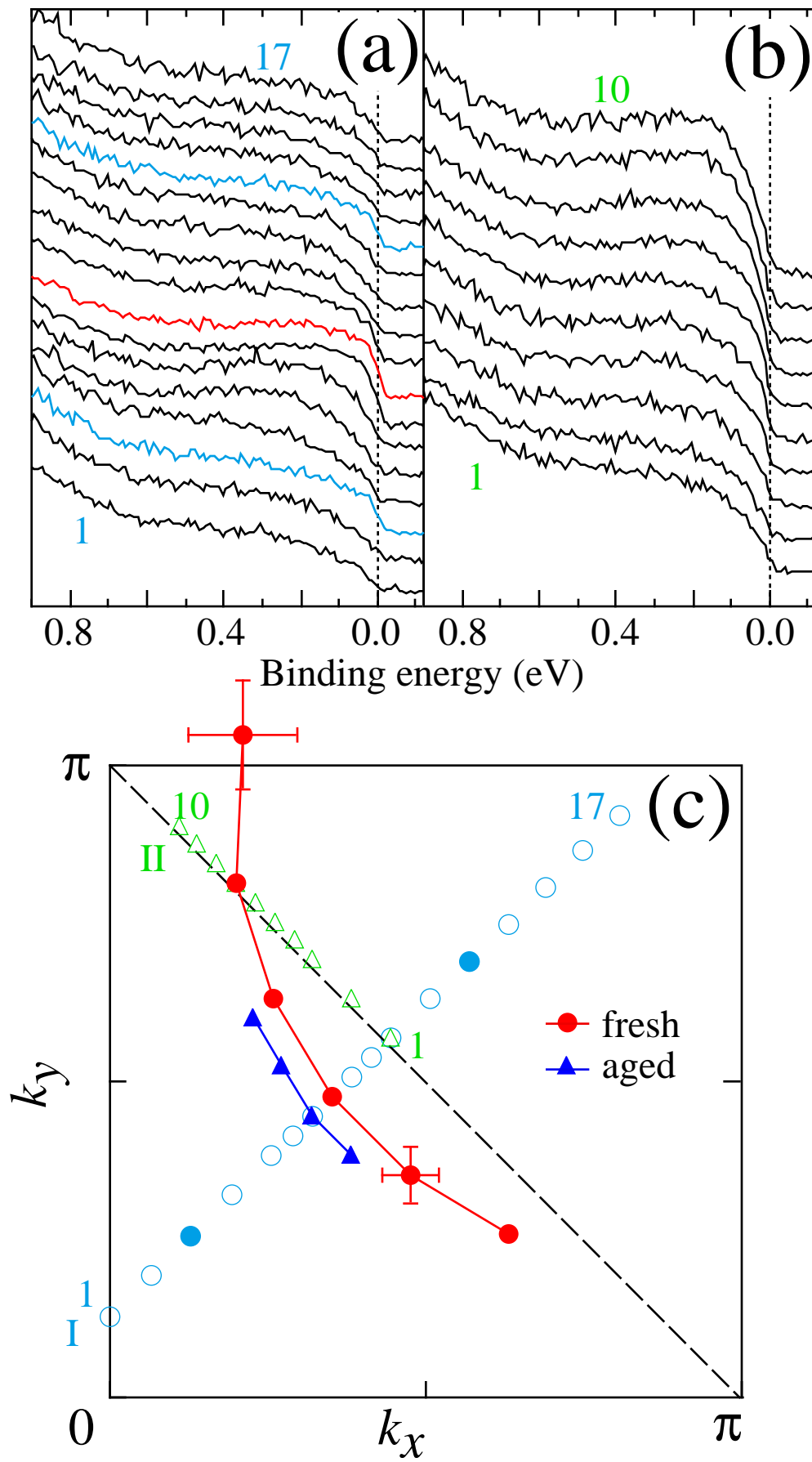


Figure 2 Ding et al

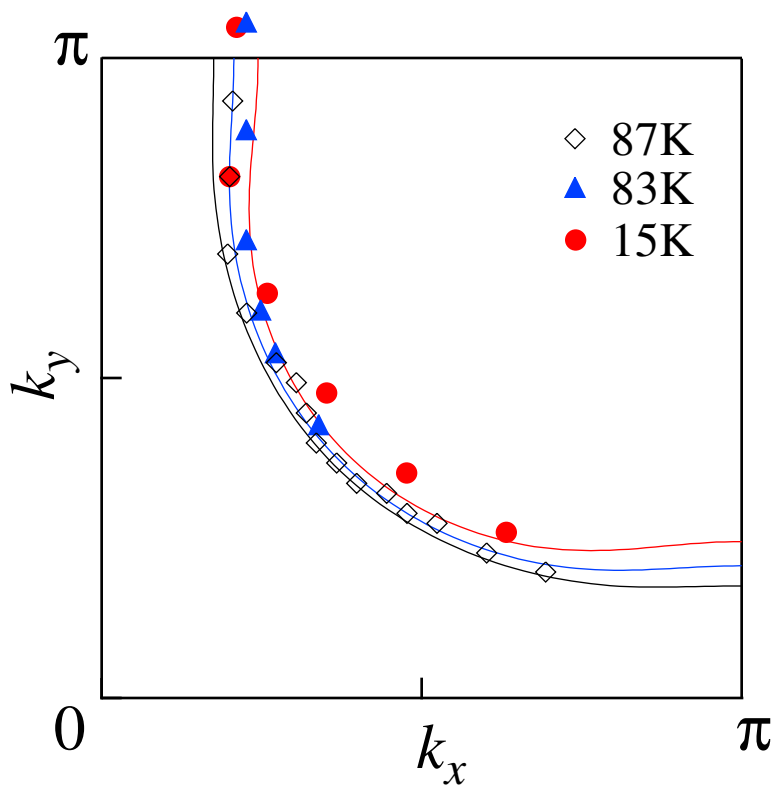


Figure 3 Ding et al.

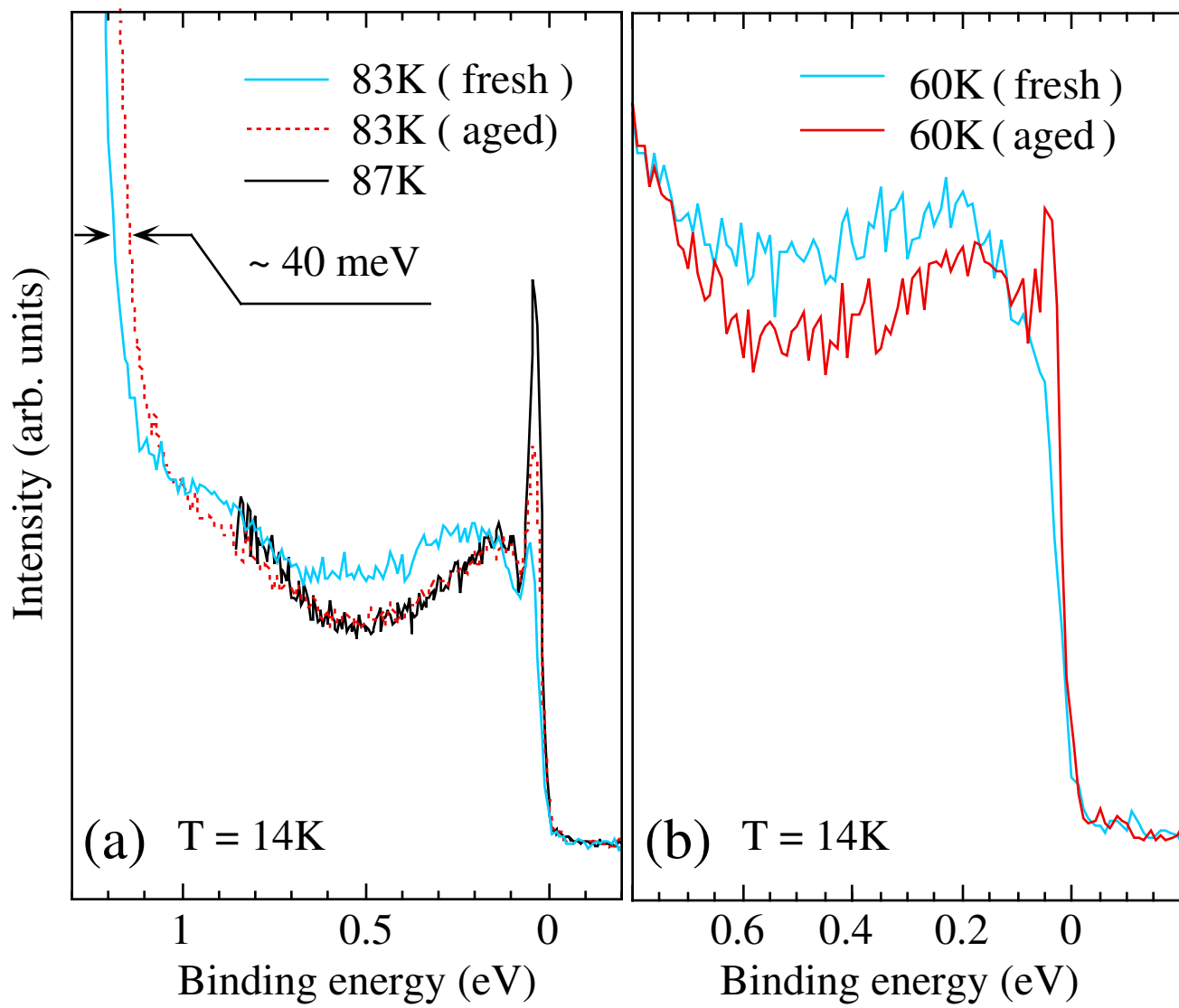


Figure 4 Ding et al.